Environ Fluid Mech (2012) 12:439–449
DOI 10.1007/s10652-012-9245-4

ORIGINAL ARTICLE

Laboratory studies defining flow regimes for negatively buoyant surface discharges into crossflow

M. Saeedi · A. Aliabadi Farahani · O. Abessi · T. Bleninger

Received: 18 September 2011 / Accepted: 21 May 2012 / Published online: 4 June 2012

Abstract Surface discharges of negatively buoyant jets into moving ambient water create a range of complex flow patterns. These complexities arise through the interplay between the discharge's initial fluxes and the motion of the ambient current. In this study a series of laboratory experiments were conducted for negatively buoyant surface discharges into crossflow to investigate flow patterns under different discharge and ambient conditions. The results compared with simulations of the CORMIX model, an expert system for ocean outfall design. In CORMIX, the simulation module DHYDRO for dense discharges has been used. Finally the flow different patterns were arranged in a dimensionless diagram to propose a modified flow classification system with new criteria.

Keywords Surface discharge · Flow regimes · Negatively buoyant · Flow pattern · CORMIX

1 Introduction

Many studies for the disposal of negatively buoyant effluents i.e. flow with densities higher than the receiving water, have been recently reported for discharges into marine coastal zones [1–5]. The higher effluent density is commonly associated with the differences in temperature, salinity and suspended solids. Examples are natural discharges of cold water inflows into lakes [6], discharges of dredging residuals [7] and brine (saline) discharges from desalination plants [8,9]. Due to the urgent need to meet freshwater demands in arid and semi-arid areas in the last decade, seawater desalination plants have grown rapidly in number and size [10].

M. Saeedi (✉) · A. A. Farahani · O. Abessi
Department of Water and Environment, School of Civil Engineering,
Iran University of Science and Technology, PO Box 16765-163, 16846 Narmak, Tehran, Iran
e-mail: msaeedi@iust.ac.ir

T. Bleninger
Department of Environmental Engineering (DEA),
Federal University of Paraná (UFPR), Curitiba, Parana, Brazil

The brine effluents produced by desalination plants are usually discharged into the nearby water body. The discharge flow rates are large, generally up to 40 % of the intake flow rate for the reverse osmosis (RO) process and up to 90 % (including cooling water) for multi-stage-flash (MSF) process. Thus, they are either almost as large or even considerably larger than the required drinking water flow rate. Regarding the fact that in some desalination plants (mostly thermal plants), saline effluents are mixed with cooling water from the process or co-generating power plants, final effluent can be positive, neutral, or negatively buoyant [11].

In order to dispose the brine into the marine environment, desalination plants use either submerged or surface discharge systems. Although, submerged systems are more efficient, they are more expensive than surface discharge systems, especially for large desalination plants (flows $>5\,m^3/s$). Therefore, in many developing countries like Iran [5,10], surface shoreline discharges are still used as a cheaper alternative [12] to dispose lightly polluted effluents which need less mixing to reach the required dilutions [14].

In surface discharges the positively buoyant flow spreads horizontally at the surface [15,16]. However, negatively buoyant surface discharge, which is the focus of this study, is characterized by a plunging motion of the effluent towards the seabed which makes the behavior of flow distinctively different from the positively buoyant one [5,17]. Studies on surface buoyant jet dynamics started in the 1960s [18,19] and have continued in 1970–1990s by Stefan et al. [20], Prych [21], Carter and Regier [22], Shirazi and Davis [23], Jones et al. [12,14], Jirka et al. [15] and Chu and Jirka [16]. In more recent studies, Jirka et al. [15] investigated the structure and mixing behavior of positively buoyant surface jets in stagnant and flowing ambient conditions. To identify jet behavior in flowing ambient, Chu and Jirka [16] conducted large series of laboratory experiments and classified the motion of positively buoyant surface jets into three distinctive regimes. Along with the results of this study, the laboratory data from Abdelwahed and Chu [24], Delft Hydraulics [25] and Brocard [26] were utilized to develop a tree-like classification scheme for surface buoyant discharges in CORMIX3 [12].

CORMIX (www.cormix.info) is an expert system to predict steady-state mixing zone properties of discharges in water bodies. CORMIX utilizes a length scale approach to classify flow regimes and series of sequential modules, CorJet for submerged discharges [27] and CorSurf for surface discharges [28] to simulate flow behavior in each of the aforementioned regimes. CORMIX3 is the surface discharge subsystem of CORMIX developed for positively buoyant flow [12]. Based on Chu and Jirka's classification diagram [16], Jones et al. [12] developed a comprehensive tree-like structure to classify surface inflows into four regimes and nine sub-regimes. Part of this classification framework was coded also for D-CORMIX [29], the subsystem developed for negatively buoyant discharges. CORMIX version 6.0 (and higher) includes the negatively buoyant simulation model DHYDRO, adapted from the previous D-CORMIX module, to simulate dense surface discharges [30]. The present study describes laboratory experiments to analyze surface dense flow regimes for different discharge and ambient conditions compared to DHYDRO simulations.

2 Prediction methodology

The features of turbulent jets can be characterized by source fluxes i.e., the initial discharge volume flux, $Q_0(=u_0A_0)$, momentum flux, $M_0(=Q_0.u_0)$, and buoyancy flux, $J_0(=Q_0.g'_0)$, where u_0 is the discharge velocity, A_0 is the discharge cross-sectional area and g'_0 is the initial reduced gravity $(=(\frac{\Delta\rho}{\rho_a}).g)$ [13,15]. Comparison of these fluxes with each other and with

characteristic ambient flow parameters, such as the velocity u_a, and/or water depth H, allows defining some characteristic length scales [31]. L_Q is the discharge length scale and defined as $L_Q = \frac{Q_0}{M_0^{1/2}}$. It measures the relative significance of the volume flux compared to the momentum flux and indicates the region where the discharge channel geometry strongly affects the flow characteristics. $L_M = \frac{M_0^{3/4}}{J_0^{1/2}}$ is jet-to-plume length scale and measures the relative importance of the initial momentum and buoyancy fluxes. L_M indicates the distance over which the buoyancy generated momentum approximately equal to discharge initial momentum flux (M). $L_m = \frac{M_0^{1/2}}{u_a}$ is the jet-to-cross flow length scale and describes the relative importance of the initial momentum to the ambient velocity. This length scale indicates the location where the flow becomes strongly deflected by the ambient flow. And finally, $L_b = \frac{J_0}{u_a^3}$ is the plume-to-cross flow length scale and measures the relative importance of initial buoyancy flux to the ambient crossflow velocity. These length scales provide a framework for interpreting the behavior of buoyant discharges in varying conditions [1].

The dependence of the physical properties of the surface discharge on the discharge and ambient characteristics can be written as follows:

$$\text{Jet property} = f(Q_0, M_0, J_0, u_a, b_0, h_0, \theta_0, H) \tag{1}$$

where, b_0 is the discharge channel width or diameter, h_0 is the water depth at the discharge outlet, θ_0 is the discharge angle and H is the ambient water depth. In terms of the length scales, Eq. 1 can be written in non-dimensional form as:

$$\text{Jet property} = f\left(\frac{L_Q}{L_M}, \frac{L_Q}{L_m}, \frac{L_M}{H}, \frac{L_Q}{H}, \frac{h_0}{b_0}, \theta_0\right) \tag{2}$$

The first ratio in Eq. 2 can be further simplified as [14]:

$$\frac{L_Q}{L_M} = \frac{\sqrt{g_0'.A_0^{1/2}}}{u_0} = \frac{1}{Fr_d} \tag{3}$$

where Fr_d is the densimetric Froude number and indicates when source buoyancy begins to dominate flow behavior [12]. Thus a small $\frac{L_Q}{L_M}$ value (or a large Fr_d) indicates a strong jet like flow, whereas a large $\frac{L_Q}{L_M}$ value (i.e. a small Fr_d) suggests the flow is dominated by buoyancy effects close to the point of discharge. Similarly, the ratio:

$$\frac{L_Q}{L_m} = \frac{u_a}{u_0} \tag{4}$$

defines the ambient to discharge velocity ratio. In this case, a large $\frac{L_Q}{L_m}$ value suggests a flow strongly influenced by the ambient motion near the source, whereas a small value suggests a strong jet-like flow near the source. The ratios $\frac{L_M}{H}$ and $\frac{L_Q}{H}$ are also shallowness parameters. These ratios exhibit the influence of the lower boundary (sea bed) on the surface jet region and are particularly important for surface discharges into shallow water. This study only considers perpendicular channels, so θ_0 can be dropped. The term $\frac{h_0}{b_0}$ represents the aspect ratio of the discharge channel. Many combinations of the length scale ratios are possible; however, presented ratios are obtained based on the analysis of data for the condition that aspect ratio and the channel area are of secondary importance. Thus, the following simplification

$$\text{Jet property} = f\left(\frac{L_Q}{L_m}, \frac{L_Q}{L_M}, \frac{L_M}{H}\right) \tag{5}$$

might be sufficient to describe the dominant phenomena [16].

Chu and Jirka [16] proposed a description of a cross-flow-shallowness interaction factor in the form of $(\frac{L_Q}{L_m}) \times (\frac{L_M}{H})^{3/2}$ and a source factor in the form of $\frac{L_Q}{L_M}$ for their preliminary classification framework for surface discharges. These factors provide a measure of the relative importance of the parameters controlling the flow behavior and form the basis to classify surface buoyant flow in to three main regimes: free jet regime, shoreline attached regime and plume like regime. The free jet regime is characterized by strong initial momentum flux relative to the ambient velocity. The discharged flow within the free jet regime is gradually deflected by the ambient current and does not interact with the near shoreline. In the shoreline attached regime, the strong ambient crossflow relative to the initial momentum flux of the discharge, deflects the flow such that it interacts dynamically with the shoreline. In the shoreline attached flow, the cross-sectional profile is not completely developed and the jet attaches to the shore due to the deflection of the flow centerline trajectory. In this regime a recirculation zone forms downstream of the outlet which reduces dilution performance of the jet within the receiving waters. This type of dynamic attachment will be encouraged in shallow waters because they further restrict the ambient fluid entrainment. Finally, the plume like regime occurs when a strongly buoyant effluent is discharged with a relatively low initial momentum flux into a slowly moving water [16]. This study investigates the definition of a criterion classifying jet regimes for surface discharges of negatively buoyant effluents based on the formerly introduced criteria by Chu and Jirka [16].

3 Experiments

3.1 Apparatus

The experiments were conducted in the environmental research laboratory of Iran University of Science and Technology (IUST), by discharging a continuous flow of brine into a towing tank (Fig. 1), 6 m long × 1.8 m wide × 1.5 m deep, filled with fresh water. Two storage tanks each with a capacity of 2201 were utilized as the source of brine and fresh water. Before starting experiments, fresh water used to establish the desired flow rate and velocity. The surface discharge configuration has been reproduced with a rectangular channel 8.6 cm wide, and depths varying from 0.95 to 2.9 cm. The discharge system released the flow horizontally (parallel to the free surface) and perpendicular to the towing direction. A 3 kW rotary pump was utilized to pump the brine from the storage tank to the channel and a calming device used between the pipe and the channel to reduce wave motions and to avoid secondary flows. This channel was 0.8 m long to obtain a fully developed turbulent flow profile and placed along the width of the tank to minimize side wall effects. The discharge flushed with the vertical bank, a 1.5 m long false wall representing the shore. The false wall was towed along with the channel connected to the trolley. The water level in the receiving tank was kept constant during the experiments using an overflow weir at the end of the tank. A calibrated conductivity probe (Model: Lutron YK-2014CD) was used to measure the salinity of the effluent in the storage tank. This probe also provides temperature measurements, which together with salinity have been used for density computations [32]. An electromagnetic flow meter (WELLTECH COPA-XE WT4300) was used to measure the flow rate in the supply pipe to the discharge channel. On the basis of water depth (h_0) in the outlet and channel width (b_0),

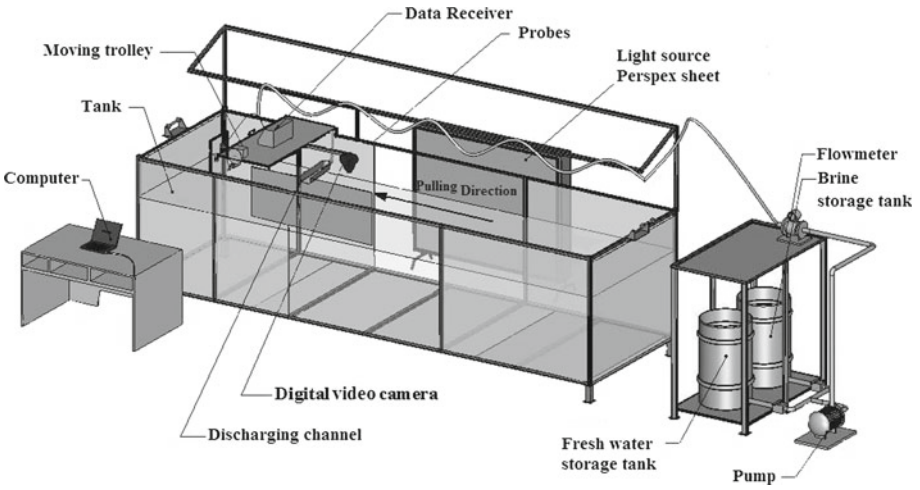

Fig. 1 Schematic diagram of experimental set up

the cross-sectional average flow velocity u_o was computed by dividing the flow rate with the cross-sectional area.

Towing the system simulates a constant ambient current, however, without the related ambient turbulence due to the absence of bottom shear in the ambient flow. The near-field turbulence induced by the discharge is much larger than the shear induced turbulence by the ambient flow. Thus, the latter can be ignored in the present study, which is only important for far-field analysis where ambient mixing becomes important. The trolley with the dimension of 0.8×1.8 m was pulled along the flume via a cable and gear system. The trolley is driven by an electric motor, an inverter, and a DC motor speed control device. Hence a wide range of trolley (current) speeds (6–80 cm/s) can be simulated. The trolley speed was calibrated by measuring its travel time between two points of known distance.

3.2 Experimental procedure

In the current study more than 130 experiments were carried out. The experiments were conducted for a wide range of average discharge velocities (7–105 cm/s) and ambient crossflow motions (6–70 cm/s). These represented velocity ratios ($\frac{u_0}{u_a}$) within the range of 0.35–7.4, typical for coastal discharges with discharge velocities varying between 0.5 and 2 m/s, and ambient velocities between 0.1 and 1 m/s. The initial discharge densimetric Froude numbers ($Fr_d = \frac{u_0}{\sqrt{g_0' \cdot A_0^{1/2}}}$) were ranging from 1.1 to 9.2 with channel Reynolds numbers ($Re = \frac{u_0 . D_H}{\nu}$ where D_H is hydraulic radius and ν is kinematic viscosity) in the range of 750–3,300. The densimetric Froude numbers are of the same order as for typical desalination plant discharges. The Reynolds number was always above 500 characterizing a fully turbulent flow regime. The ambient to discharge depth ratio ($\frac{H}{h_0}$) varied from 23 to 74 for the experiments. Large values of $\frac{H}{h_0}$ ratio show that the lower boundary (ambient floor) is not expected to have influence on the surface jet. The towing tank was filled with tap water with density equal to 0.998 $\frac{g}{cm^3}$ up to depths of 66 cm. Brine density varied within the range of 1.007–1.062 $\frac{g}{cm^3}$ for the salinities of 14–85 ppt and temperatures ranging from 20 to 24 °C resulting in a range

Table 1 Ranges of experimental parameters for discharged flow and ambient water

Discharge characteristics			Receiving water characteristics			Calculated ratios				
u_0 (cm/s)	h_0 (cm)	ρ_0 (g/cm^3)	u_a (cm/s)	H_0 (cm)	ρ_a (g/cm^3)	Fr_d	Re (channel)	H/h_0	$\frac{u_0}{u_a}$	$\Delta\rho$ (g/cm^3)
7–105	0.9–2.9	1.007–1.062	6–70	66	0.998	1.1–9.2	750–3300	23–74	0.35–7.4	9–64

of density differences, $\Delta\rho = 9$–$64\ \frac{g}{cm^3}$. Table 1 summarizes the experimental ranges for the parameters of discharged flow and ambient water and the calculated ratios.

A black soluble dye was added to the source fluid as a tracer. For each experiment a video sequence was recorded using a digital camcorder mounted directly above the discharge on the trolley. During the tests, the dye colored salt water was discharged at a constant flow rate and concentration. The image sequence was then time-averaged and processed to analyze the flow behavior. To differentiate between the flow regimes, photos of the experiments were analyzed with the image processing software, image stream [33]. Image stream produces color cell photos with contour values for light intensity in which colors varied according to the black dye tracer concentration. In this study flow patterns were investigated from top view, while no observations were made from the side view. This means that the imaged flows were integrated in a two dimensional, while the flow actually follows a three dimensional (3D) trajectory.

The coordinate system has its origin in the middle of the discharge when the x positive values increase into the direction of the ambient current. The y positive values extend up to the right while looking downstream and z is oriented downwards to the floor. Thus, from top view flow 3D trajectory integrated in the x–y plane. To check if the determination of flow regime on top plane view reflects flow three dimensional behavior properly, some 3D experiments were conducted. The experiments showed that the integration of a flow behavior in 2D would be a good estimation for the discharge in vertical bank shore, however, would be not for the surface dense discharge in slopping shore.

4 Results and discussion

Negatively buoyant surface discharge initially creates a jet moving along the free surface. In crossflow immediately after discharge, the jet flow starts interacting with the ambient flow. So the jet is deflecting by the current until following the motion of the flow. Depending on the initial buoyancy and momentum fluxes, bending occurs either before or after the jet starts plunging down to the floor. For surface discharges of dense jets in crossflow, two main flow patterns i.e. free jet and shoreline attached jet, were observed due to the complex range of hydraulic processes involved [5]. In Fig. 2, the results of image processing for three individual experiments including, free jet regimes (Fig. 2a) and shoreline attached regime (Fig. 2b, c), are shown. As illustrated in Fig. 2a, for some experiments it is easy to distinguish the flow regimes; however, for others it is not (Fig. 2b, c). Shoreline attached regimes are defined when the plume's edge contacts the bank. Thus, cross-sectional profiles are not fully developed (i.e. not Gaussian like) compared to the completely developed (i.e. fully Gaussian) profile in free jets. In this study, a criterion similar to the one utilized by Jirka et al. [15] has been used to distinguish between both regimes. Flows that laterally develop up to 10 % of the centerline intensity close to the bank shore were defined as the free jet flow. Consequently, the flows that

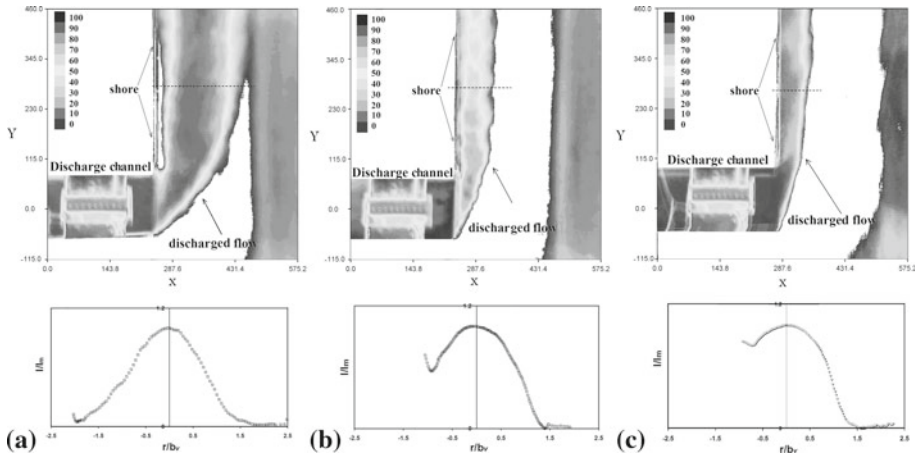

Fig. 2 Top view of time averaged pictures of experimental results after image processing and cross-sectional plot of light intensity values. **a** free jet regime, **b** shoreline attached regime, **c** shoreline attached regime; *dark part* shows light maximum intensity and *bright part* shows minimum intensity

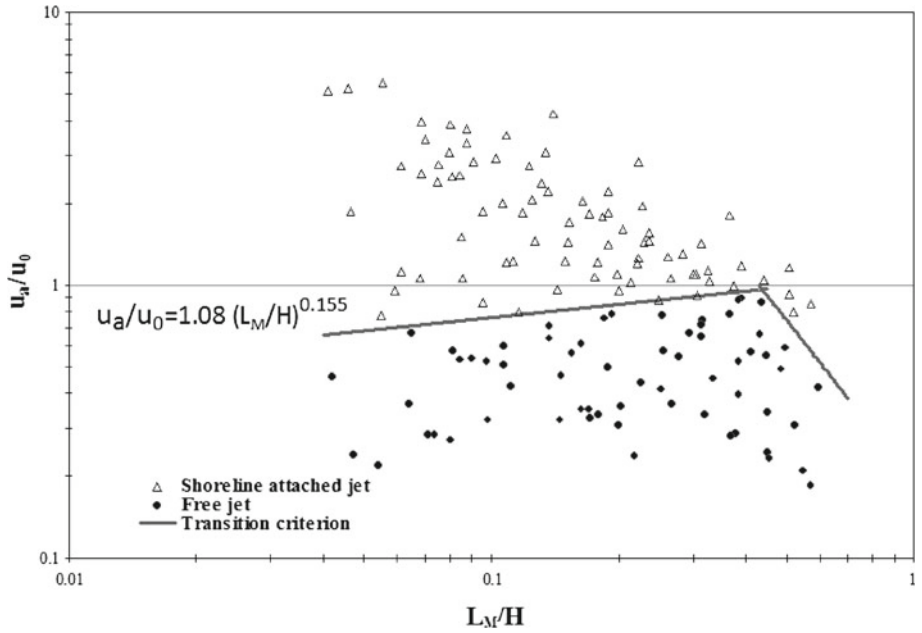

Fig. 3 Classification diagram for negatively buoyant surface discharges based on experimental observation

have been less developed in cross-sections alongshore (i.e. less than 10 %) were considered as shoreline attached flows.

Figure 3 illustrates the classification of flow regimes for each experiment, plotting $\frac{L_M}{H}$ versus $\frac{u_a}{u_0}$, based on the approach described above. For large velocity ratios ($\frac{u_a}{u_0}$) the flow is strongly influenced by the ambient motion immediately after the discharge, whereas small values suggest a strong jet-like flow near the source. The shallowness parameter ($\frac{L_M}{H}$) also correlates with the jet maximum depth and exhibits possible influences of lower boundaries

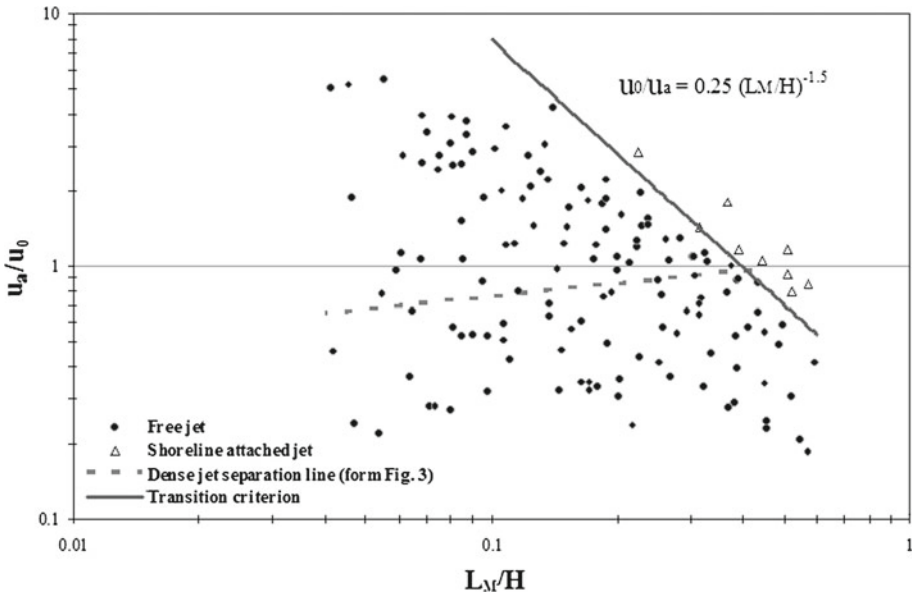

Fig. 4 Classification diagram for negatively buoyant surface discharges based on DHYDRO predictions

in the surface jet flows [12]. Based on the earlier definition, the ratios differentiate free jet flow from shoreline attached flow.

The line in Fig. 3 separating the free jet from the shoreline attached jet regime, is defined by:

$$\frac{u_a}{u_0} = 1.08 \times \left(\frac{L_M}{H}\right)^{0.155} \rightarrow \frac{u_a}{u_0} \times \left(\frac{L_M}{H}\right)^{-0.155} = 1.08 \tag{6}$$

DHYDRO, the subsystem of CORMIX specialized for discharges of dense effluents, was run for the same discharge and ambient conditions. The model input was executed for unstratified and also deep ambient water to avoid plume interactions with the lower boundary (ambient floor). The parameters utilized were obtained from the experiments and flow predicted regime for each identified. The classification diagram resulting from DHYDRO simulations is then plotted as Fig. 4.

The line that distinguishes free jet from shoreline attached jets in Fig. 4 is:

$$\frac{u_a}{u_0} = 0.25 \times \left(\frac{L_M}{H}\right)^{-1.5} \rightarrow \frac{u_a}{u_0} \times \left(\frac{L_M}{H}\right)^{1.5} = 0.25 \tag{7}$$

This criterion is consistent with the one proposed by Chu and Jirka [16] for positively buoyant discharge classification ($(\frac{L_Q}{L_m}) \times (\frac{L_M}{H})^{3/2}$), which also has been used for negatively buoyant surface discharges in the DHYDRO [29,30]. The dashed line in Fig. 4 represents the result from the experiments as of Fig. 3 for dense discharges. Comparing the power magnitude of $\frac{L_M}{H}$ in Eqs. 6 and 7, it is clear that the importance of $\frac{L_M}{H}$, distinguishing between flow regimes, for negatively buoyant discharge is considerably less than for positively buoyant discharges. It is also worth noting that the power sign of $\frac{L_M}{H}$ in Eq. 6 is negative while it is positive in Eq. 7. This indicates that for negatively buoyant discharge any decrease in L_M/H (i.e. increases in discharge density or decreases of flow velocity for fixed ambient depth)

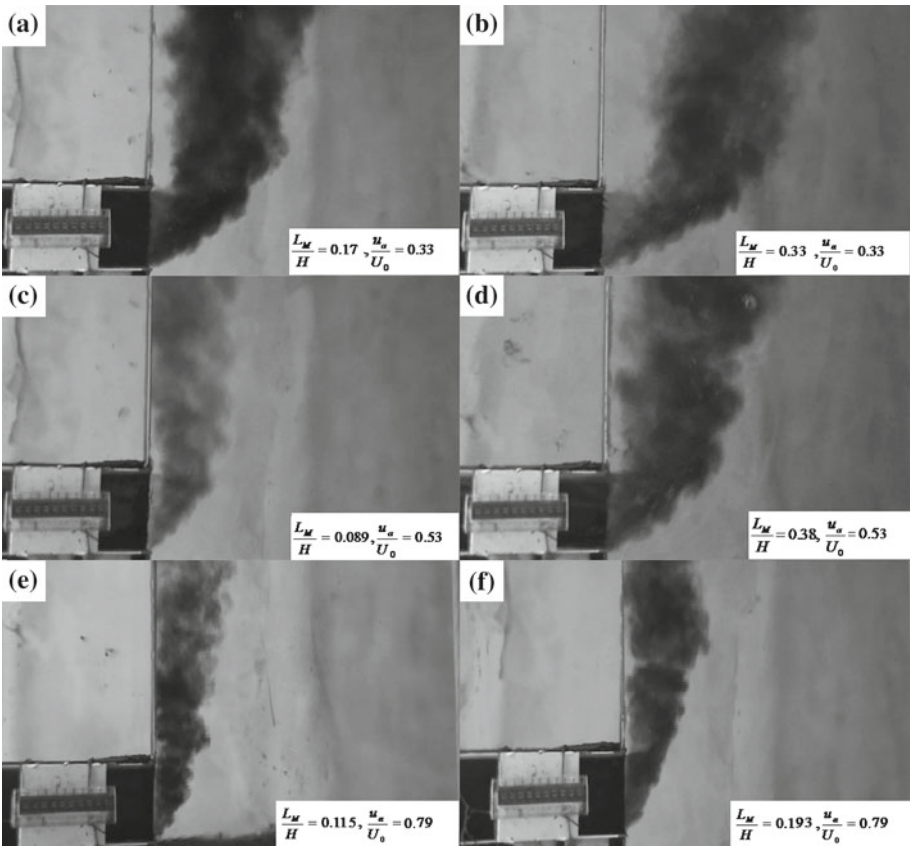

Fig. 5 Unprocessed photographs of experiments with equal $\frac{u_a}{u_0}$ and different $\frac{L_M}{H}$, in *two first pairs* distancing of flow form bank shore are shown for free jet regimes when $\frac{L_M}{H}$ increases and in *third pair*, regime changes form shoreline attached to free jet are exhibited when $\frac{L_M}{H}$ increases

facilitates the occurrence of shoreline attached jets. However, for surface positively buoyant jets, decrease in $\frac{L_M}{H}$ promotes occurrences of free jets. The influences of changing $\frac{L_M}{H}$ in the behavior of surface dense flow are illustrated in series of photos in Fig. 5. The figure shows experiments with identical $\frac{u_a}{u_0}$ and varying $\frac{L_M}{H}$. Increases in $\frac{L_M}{H}$ (from left to right) generally led to increases of the distance of the plume from the shore. Similarly, decreases of $\frac{L_M}{H}$, for the condition that H, u_0 and u_a are constant and only the discharge density (ρ_0) increases, promote formations of shoreline attached jets as a result of slight increases in the surface jet maximum depth.

Comparing Figs. 3 and 4, three areas can be identified as shown in Fig. 6. The first zone (black circle, ●) is the area where CORMIX predictions and experimental observations are in agreement with predicting free jets. The second (white triangle, Δ) is the area where CORMIX prediction and experimental observations were in agreement with predicting shoreline attached jets. The third area (black square, ■) is the area that CORMIX predictions were free jet but the experiment observations are shoreline attached jet. In the shoreline attached flow, recirculation restricts mixing and entrainment. Hence, these results provide an evidence on

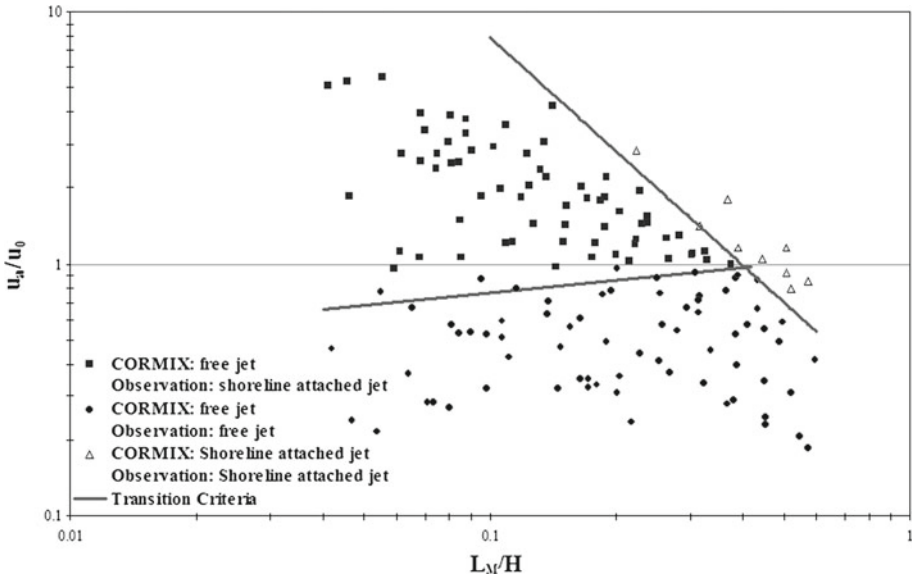

Fig. 6 Flow comparative classification diagram in surface discharge of negatively buoyant jet

how to improve the CORMIX classification to avoid the over estimation of dilution in those cases.

5 Conclusions

Extensive series of experiments have been conducted to investigate the flow regimes of negatively buoyant surface discharges into crossflow under a variety of discharge and ambient flow conditions. The experiments were utilized to develop a classification diagram to distinguish between the free jet and the shoreline attached jet. Those results have been compared with the result of DHYDRO simulation from the CORMIX model. Comparisons showed that they exhibited the opposite role of the criterion $\frac{L_M}{H}$ for negatively and positively buoyant discharges. General comparison of the regimes observed in laboratory and predicted by DHYDRO exhibited three different zones where CORMIX predictions are either compatible or inconsistent with the observations. The new determined criterion can be used to improve the CORMIX classification diagram for surface dense jets to avoid the over estimation of dilution in the area that it suggests free jet and is not, as well as for screening analysis of environmental impact assessments.

Acknowledgments The authors acknowledge the comments and support given by Dr. Robert Doneker related to the CORMIX methodology, as well as the provided software access.

References

1. Doneker RL, Jirka GH (2001) CORMIX-GI systems for mixing zone analysis of brine waste water disposal. Desalination 139:263–274
2. Purnama A, Al-Barwani HH, Al-Lawatia M (2003) Modeling dispersion of brine waste from a coastal desalination plant. Desalination 155:41–47

3. Bleninger T, Jirka GH (2008) Modeling and environmentally sound management of brine discharges from desalination plants. Desalination 221:585–597
4. Shao D, Law AWK (2010) Mixing and boundary interactions of 30° and 45° inclined dense jets. Environ Fluid Mech 10:521–553
5. Abessi O, Saeedi M, Davidson M, HajizadehZaker N (2011) Flow classification of negatively buoyant surface discharge in an ambient current. J Coastal Res. doi:10.2112/JCOASTRES-D-10-00131.1
6. Robert HS, Gibbs M, Waugh B (2005) Field calibration of a formula for entrance mixing of river inflows to lake: Lake Taupo, North Island, New Zealand. New Zeal J Mar Fresh 39:785–802
7. Roberts PJW, Tome G (1987) Inclined dense jets in flowing current. J Hydraul Eng 113:323–341
8. Roberts PJW, Ferrier A, Daviero G (1997) Mixing in inclined dense jet. J Hydraul Eng 123:693–699
9. Kikkert G, Davidson M, Nokes I (2007) Inclined negatively buoyant discharges. J Hydraul Eng 133:545–554
10. Ahmed M, Shayya WH, Hoey D, Al-Handaly J (2001) Brine disposal from reverse osmosis desalination plants in Oman and the United Arab Emirates. Desalination 133:135–147
11. Bleninger T, Niepelt A, Jirka GH (2010) Desalination plant discharge calculator. Desalination Water Treat 13:156–173
12. Jones RG, Nash DJ, Jirka HG (1996) CORMIX3: an experimental system for mixing zone analysis and prediction of buoyant surface discharges. Cornell University, User manual, DeFrees Hydraulics Laboratory, New York
13. Lattemann S, Hopner T (2003) Seawater desalination: impacts of brine and chemical discharges on the marine environment. Desalination Publ, L'Aquila, p 142. ISBN:0–6689–062–9
14. Jones G, Nash D, Doneker L, Jirka H (2007) Buoyant surface discharge into water bodies. I: flow classification and prediction methodology. J Hydraul Eng 133:1010–1020
15. Jirka GH, Adams EE, Stolzenbach KD (1981) Buoyant surface jets. J Hydraul Div 107:1467–1487
16. Chu VH, Jirka GH (1986) Chapter 25: surface buoyant jets, encyclopedia of fluid mechanics. Gulf Publishing Company, Houston, p 155
17. Kassem A, Imran J (2001) Simulation of turbid underflows generated by the plunging of a river. Geology 29(7):655–658
18. Jen Y, Wiegel RL, Mobarek I (1966) Surface discharges of horizontal warm water jets. Power Div 92:1–29
19. Motz LH, Benedict BA (1970) Heated surface jet discharged into a flowing ambient stream. Vanderbilt University, Department of Environmental and Water Resources Engineering, Nashville (Tech. Rep. 4)
20. Stefan H, Hayakawa N, Schiebe FR (1971) Surface discharge of heated water. U.S. Environmental Protection Agency, Washington, DC (Rep. 16130)
21. Prych EA (1972) A warm water effluent analyzed as a buoyant jet. Sverigas Meteorologiska och Hydrologiska Institut, vol. 21. Service Hydraulique, Stockholm
22. Carter HH, Regier R (1974) The three-dimensional heated surface jet in a crossflow. Johns Hopkins University, Chesapeake Bay Institute, Baltimore, p 50 (Tech. Rep. 88)
23. Shirazi MA, Davis LR (1974) Workbook on thermal plume prediction. U.S. Environmental Protection Agency, Corvallis. Technical Series, 2-surface discharges (Tech. Rep. EPA-R2-72-0056)
24. Abdelwahed MST, Chu VH (1981) Surface jets and surface plumes in crossflows. McGill University, Fluid Mechanics Laboratory, Montreal, p 120 (Tech. Rep. 81–1)
25. Delft Hydraulics (1983) Buoyant surface jets in crossflow. Delft Hydraulics Laboratory, Delft, p 210. Report on experimental investigation-S350-II
26. Brocard DN (1984) Surface buoyant jets in reversing and steady crossflows. 1: experiments. Alden Research Laboratory, Worcester, p 80 (Tech. Rep. 18-84/M424F)
27. Jirka GH (2004) Integral model for turbulent buoyant jets in unbounded stratified flows. Part 1: single round buoyant jet. Environ Fluid Mech 4(1):1–56
28. Jirka GH (2007) Buoyant surface discharges into water bodies. II: jet integral model. J Hydraul Eng 133(9):1021–1036
29. Doneker LR, Jirka GH (1997) D-CORMIX continues dredge disposal mixing zone water quality model laboratory and filed data validation study. U.S. environmental protection agency, Washington, DC.
30. Doneker RL, Jirka GH (2007) CORMIX user manual: a hydrodynamic mixing zone model and decision support system for pollutant discharges into surface waters. U.S.EPA-823-K-07-001
31. Fischer B, List JE, Imberger J, Brooks HN (1979) Mixing in inland and coastal waters. Academic Press, Inc., New York, p 212
32. Millero FJ, Poisson A (1981) International one atmosphere equation of state for sea water. Deep sea Res 13:453–459
33. Nokes RI (2005) ImageStream version 4.01. University of Canterbury. Image Processing Software, Christchurch